Effects of vacancies in the Hubbard models on several chains and ladders

1999 J. Phys.: Condens. Matter 11 493

(http://iopscience.iop.org/0953-8984/11/2/014)

J. Phys.: Condens. Matter **11** (1999) 493–512. Printed in the UK PII: S0953-8984(99)96481-0

Effects of vacancies in the Hubbard models on several chains and ladders

H Asakawa
The Institute of Physical and Chemical Research (RIKEN), Wako, Saitama 351-0198, Japan

Received 4 August 1998, in final form 5 October 1998

Abstract. The effects of vacancies (i.e. chargeless and spinless impurities) in the Hubbard models on several chains and ladders are studied; these latter are simple and dimerized chains, and standard and zigzag two-leg ladders. Local electron numbers and local magnetizations near the vacancies are evaluated by the quantum Monte Carlo method.

1. Introduction

Recently, the effects of nonmagnetic impurities in low-dimensional quantum spin systems have attracted much attention. Through intensive studies by many authors (see, e.g., references [1–4], the behaviours near the impurity (i.e. vacancy) in the Heisenberg models on various lattices have been clarified. See, e.g., [5] and references cited therein.

In the present paper, we study the Hubbard model with a chargeless and spinless impurity (i.e. vacancy), as an extension of the Heisenberg model with a vacancy. As a result of this extension, we have not only the spin degree of freedom but also the charge degree of freedom. We discuss charge and spin properties near the vacancy for the Hubbard models on several chains and ladders, by using the quantum Monte Carlo method.

Since we are interested in the relationships between the impurity effects and the bulk properties, we choose the lattice configurations and the parameters in the Hubbard models such that the present models realize various states in the bulk, e.g. band insulators and Mott insulators with or without spin gaps.

The purpose of the present work is to achieve an understanding of the variety of effects of the impurity in the Hubbard model.

2. The model

In the present paper, we consider the effects of vacancies in the Hubbard model on several lattices, described by

$$\mathcal{H} = -\sum_{\langle i,j\rangle} t_{ij} \sum_{\sigma=\pm} (c^{\dagger}_{i\sigma} c_{j\sigma} + c^{\dagger}_{j\sigma} c_{i\sigma}) + 4u \sum_{j} \left(n_{j+} - \frac{1}{2} \right) \left(n_{j-} - \frac{1}{2} \right) \qquad (2.1)$$

where $c_{j\sigma}$ (or $c^{\dagger}_{j\sigma}$) denotes the annihilation (or creation) operator at site j with spin σ and $n_{j\sigma}$ stands for a number operator defined by $n_{j\sigma} \equiv c^{\dagger}_{j\sigma} c_{j\sigma}$. The sum $\sum_{\langle i,j\rangle}$ runs over all of the pairs of sites on the bonds of the lattice, while $\sum_j$ runs over all of the sites. We introduce a chargeless and spinless impurity at site j_0 by removing the operators of the site.

0953-8984/99/020493+20$19.50

Since the Hubbard model at half-filling approaches the Heisenberg model for the limit $u \to \infty$, our model (2.1) with vacancies can be recognized as an extension of the Heisenberg spin system with nonmagnetic impurities.

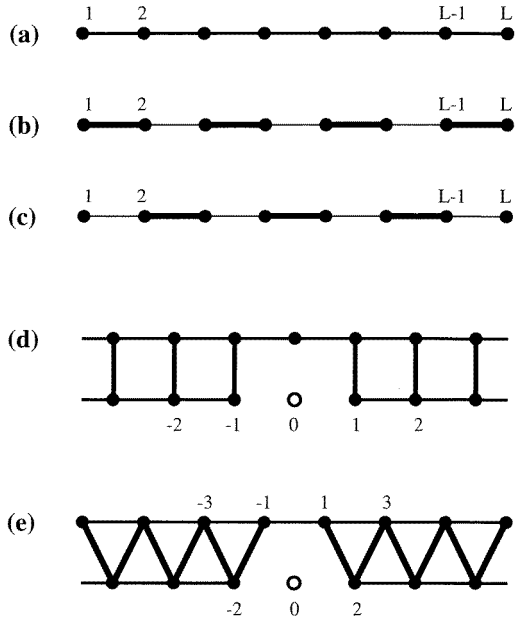

Figure 1. Cluster geometries for the Hubbard model with vacancies; (a) an ordinary open chain (section 3), (b) a type-A bond-alternating open chain (section 4), (c) a type-B bond-alternating open chain (section 4), (d) a two-leg ladder with a vacancy (section 5) and (e) a zigzag ladder with a vacancy (section 6).

In section 3, we discuss the ordinary Hubbard chain in order to explain our strategy. The bond-alternating Hubbard chain with spinless and chargeless impurities is studied in section 4. We also study the effects of vacancies in the two-leg Hubbard ladder and in the zigzag Hubbard ladder, in sections 5 and 6. We focus on the cases of almost half-filling in each model. The cluster geometries of these models are shown in figure 1.

Before closing this section, we need to make a short comment, as a preliminary for later discussions. We remark that the present system has the SO(4) symmetry when the relevant lattice is bipartite [6]. In fact, the six generators of the symmetry are given by

$$S^+ = \sum_j c^\dagger_{j+} c_{j-} \qquad S^- = (S^+)^\dagger \qquad S^3 = \frac{1}{2}\sum_j (n_{j+} - n_{j-}) \tag{2.2}$$

$$T^+ = \sum_j \epsilon_j c_{j+} c_{j-} \qquad T^- = (T^+)^\dagger \qquad T^3 = \frac{1}{2}\sum_j (1 - n_{j+} - n_{j-}) \tag{2.3}$$

where the sum $\sum_j$ runs over all of the sites, and ϵ_j takes the value 1 (or -1) when the site j belongs to the A (or B) sublattice. Each of the sets $\{S^+, S^-, S^3\}$ and $\{T^+, T^-, T^3\}$ realizes the generators of the SU(2) symmetry in the spin and charge sectors, respectively. Therefore, we can express the symmetry as $\mathrm{SO}(4) = \mathrm{SU}(2)_{\mathrm{charge}} \times \mathrm{SU}(2)_{\mathrm{spin}}/\mathrm{Z}_2$. We describe the total spin (or the z-component of the total spin) by the symbol S (or S^z). We use the symbols T and T^z to express the corresponding quantum numbers in the charge sector.

3. The Hubbard open chain

In the present section, we explain how to understand the properties of the region around the vacancy in the Hubbard models. For this purpose, we take the one-dimensional ordinary Hubbard model as an example; it is described by

$$\mathcal{H} = -t \sum_{j} \sum_{\sigma=\pm} (c^{\dagger}_{j\sigma} c_{j+1\sigma} + c^{\dagger}_{j+1\sigma} c_{j\sigma}) + 4u \sum_{j} \left(n_{j+} - \frac{1}{2} \right) \left(n_{j-} - \frac{1}{2} \right). \tag{3.1}$$

By eliminating the operators at a site, we introduce a chargeless and spinless impurity at the site. Such a impurity cuts the chain, so we can recognize the effects of the impurities as those of the boundaries. On the other hand, since an impurity does not cut ladder-type systems, impurity effects do not necessarily mean boundary effects.

We calculate the reduced local densities of charge and spin sectors:

$$\chi^{(\mathrm{c})}(x) = -\frac{1}{2} \langle n_{x+} + n_{x-} - 1 \rangle \qquad \text{and} \qquad \chi^{(\mathrm{s})}(x) = \frac{1}{2} \langle n_{x+} - n_{x-} \rangle. \tag{3.2}$$

We evaluate $\chi^{(\mathrm{c})}$ for $(N_+, N_-) = (\frac{L}{2} - 1, \frac{L}{2} - 1)$ (or $=(\frac{L}{2} - \frac{1}{2}, \frac{L}{2} - \frac{1}{2})$) and $\chi^{(\mathrm{s})}$ for $(N_+, N_-) = (\frac{L}{2} + 1, \frac{L}{2} - 1)$ (or $=(\frac{L}{2} + \frac{1}{2}, \frac{L}{2} - \frac{1}{2})$) when the chain length L is even (or odd). Here, we describe the numbers of the electrons with up and down spins by the symbols N_+ and N_-, respectively. We remark that $\chi^{(\mathrm{c})}(x) = \chi^{(\mathrm{s})}(x)$ holds for $u = 0$. We may recognize $\chi^{(\mathrm{s})}(x)$ as the local density of two particles (or one particle) for even (or odd) L. Each particle has spin $+\frac{1}{2}$ and charge 0 (i.e. $S^z = \frac{1}{2}$, $T^z = 0$ in terms of the SO(4) symmetry) and is called a 'spinon'. Similarly, $\chi^{(\mathrm{c})}(x)$ stands for the local density for the two-particle (or one-particle) state when L is even (or odd). Such a particle has charge $+\frac{1}{2}$ and spin 0 (i.e. $T^z = \frac{1}{2}$, $S^z = 0$) and is called a 'holon'. We may also name the particles with quantum numbers of opposite signs the 'antispinon' and the 'antiholon', respectively. See, e.g., reference [7].

In order to evaluate the local densities, we use the quantum Monte Carlo method [8] of the auxiliary-field scheme for canonical ensembles [9–11]. We take $T/t = 0.1$ as the temperature. Then, we recognize that the systems almost realize the ground-state properties. Extrapolating the data for various Trotter numbers, we obtain the results for the relevant quantum systems. For each simulation, we take 10 000 steps for relaxations and 100 000 steps for measurements. The results thus obtained are shown in figure 2. We have taken the parameters $L = 59$, 60 and $u/t = 0.5$. Typical errors ($\sim 1\ \sigma$) are less than the symbol sizes. (We have also performed similar numerical calculations in the following sections.)

We also plot the uniform part χ_{u} and the alternating part χ_{a} of the local densities χ (i.e. $\chi^{(\mathrm{c})}$ or $\chi^{(\mathrm{s})}$), which are defined as

$$\chi(x) = \chi_{\mathrm{u}}(x) - (-1)^x \chi_{\mathrm{a}}(x).$$

In our numerical calculations, we have estimated $\chi_{\mathrm{u,a}}$ by [5]

$$\chi_{\mathrm{u}}(x) \simeq \frac{1}{2}\chi(x) + \frac{1}{4}(\chi(x+1) + \chi(x-1))$$

and

$$\chi_{\mathrm{a}}(x) \simeq (-1)^x (\chi_{\mathrm{u}}(x) - \chi(x)).$$

We can recognize $\chi_{\mathrm{u}}(x)$ as the average density of holes or spins at x. The magnitude of the staggered structure is described by $\chi_{\mathrm{a}}(x)$. While the staggered structure in the spin sector corresponds to '$\cdots + - + - + \cdots$', that for the charge sector is given by '$\cdots 0 \pm 0 \pm 0 \cdots$'.

The behaviour of the spin sector is qualitatively the same as that of the Heisenberg open chain; see, e.g., reference [5].

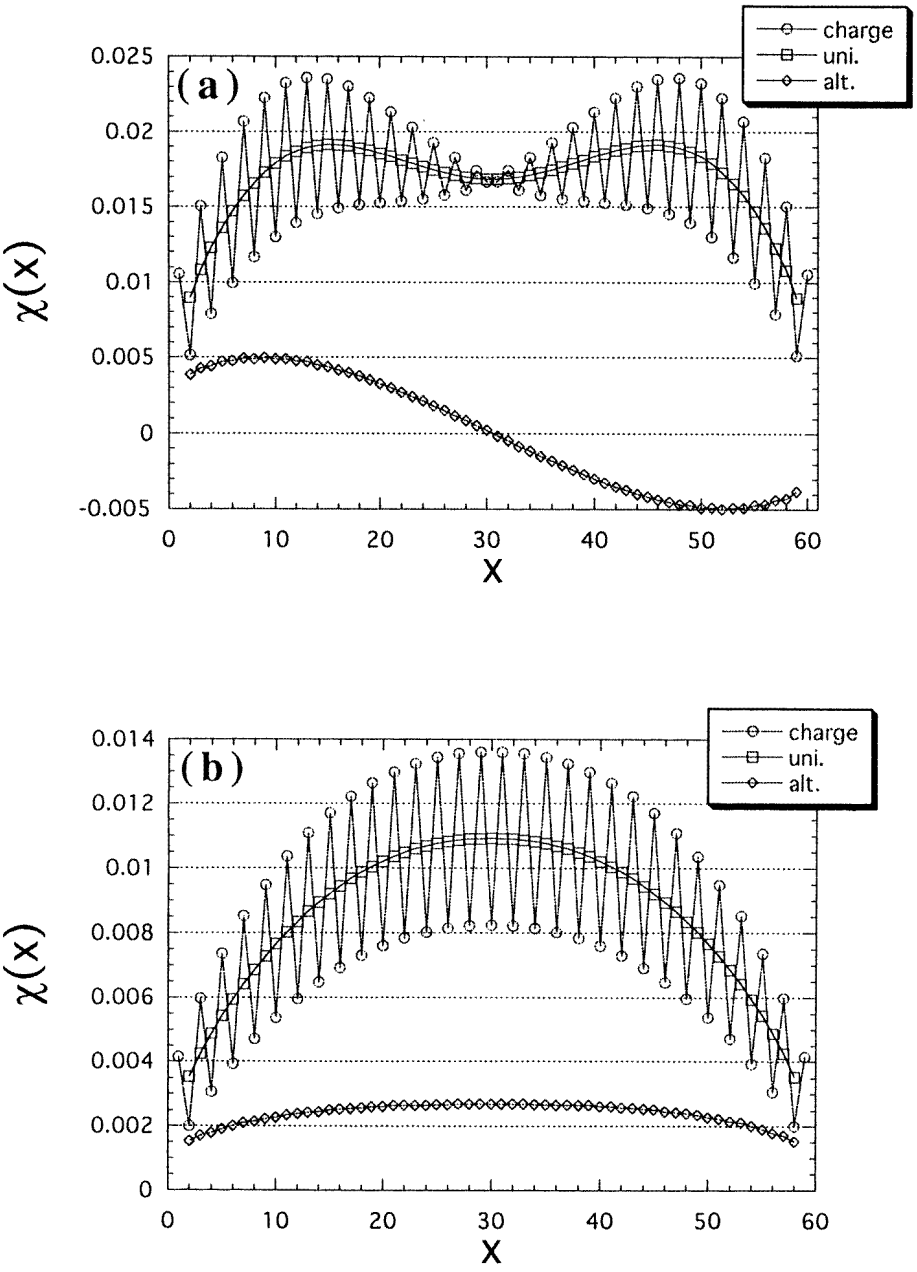

Figure 2. Local densities of the charge and spin sectors in the Hubbard open chain. The charge local density $\chi^{(c)}(x)$ and its uniform part and alternating part are shown for each of the cases: (a) $T^z = 1$, $S^z = 0$ ($L = 60$) and (b) $T^z = \frac{1}{2}$, $S^z = 0$ ($L = 59$). The spin local density $\chi^{(s)}(x)$ and its uniform part and alternating part are given for each of the cases (c) $T^z = 0$, $S^z = 1$ ($L = 60$) and (d) $T^z = 0$, $S^z = \frac{1}{2}$ ($L = 59$).

Under the open boundary condition, the Hubbard model can be solved exactly by the Bethe-*ansatz* method [12]. However, it is difficult to evaluate the local physical quantities

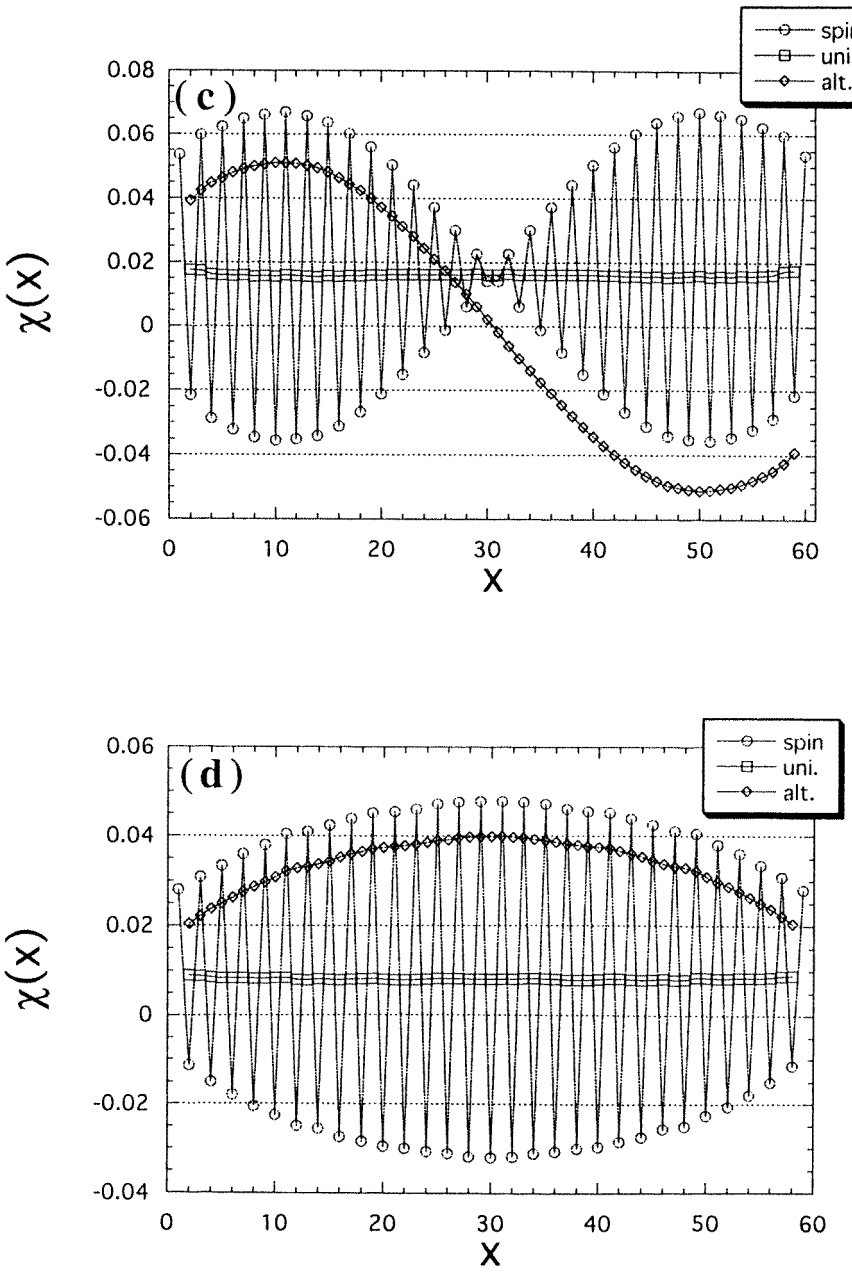

Figure 2. (Continued)

using the Bethe-*ansatz* wave function; refer to [13]. (Bedürftig *et al* [14] have evaluated local quantities in the Hubbard open chain away from half-filling, by using the density matrix renormalization group method.) If we use the bulk [7] and the boundary [15] scattering matrices of the holon and the spinon, we may be able to evaluate such quantities as $\chi^{(c)}(x)$ and $\chi^{(s)}(x)$ in the thermodynamic limit, analytically.

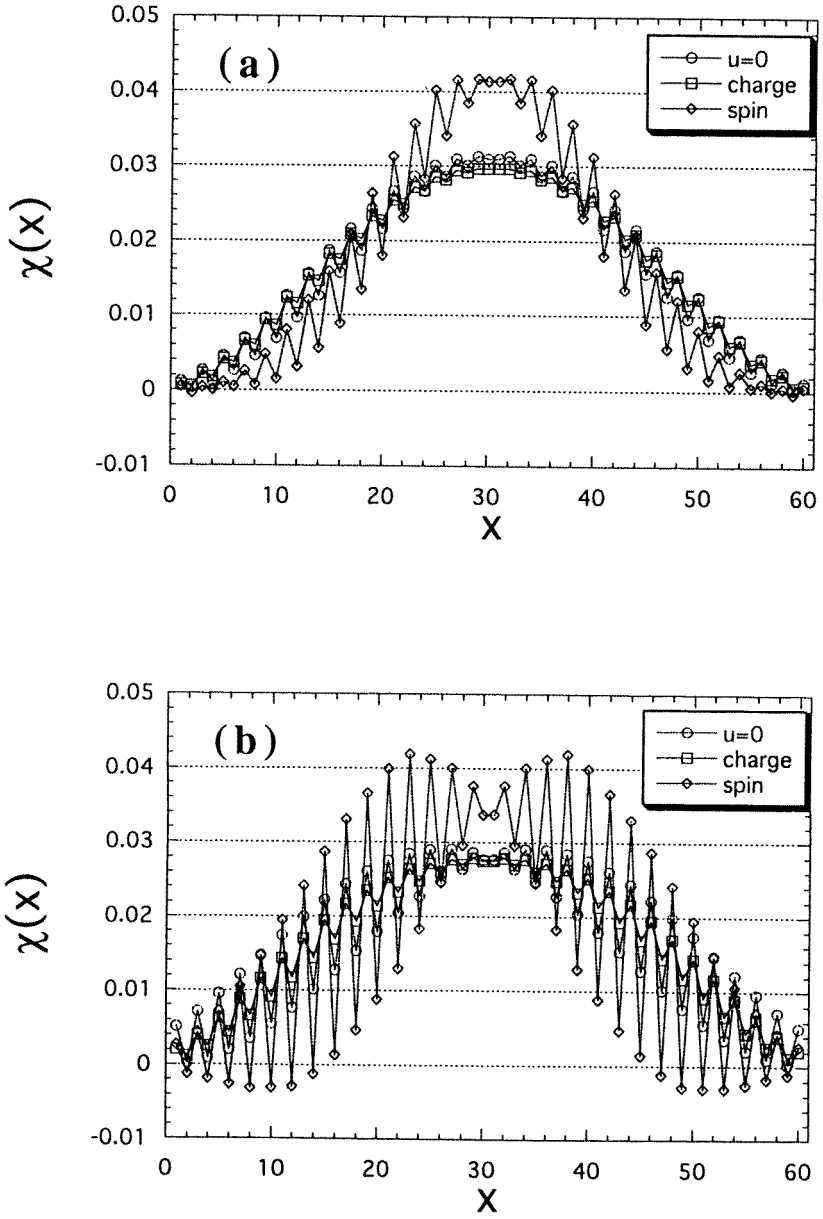

Figure 3. Local densities of the charge and spin sectors in the bond-alternating Hubbard chain with $L = 60$. The charge ($\chi^{(c)}(x)$) and the spin ($\chi^{(s)}(x)$) local densities are evaluated for $T^z = 1$, $S^z = 0$ and for $T^z = 0$, $S^z = 1$, respectively. The results for the type-A model with $r = 0.5$ (or $r = 0.8$) are given in panels (a) (or (b)), while the results for the type-B model with $r = 0.5$ (or $r = 0.8$) are also given, in panels (c) (or (d)).

4. The bond-alternating chain with boundaries

In the present section, we consider effects of chargeless and spinless impurities in the bond-alternating Hubbard chain described by

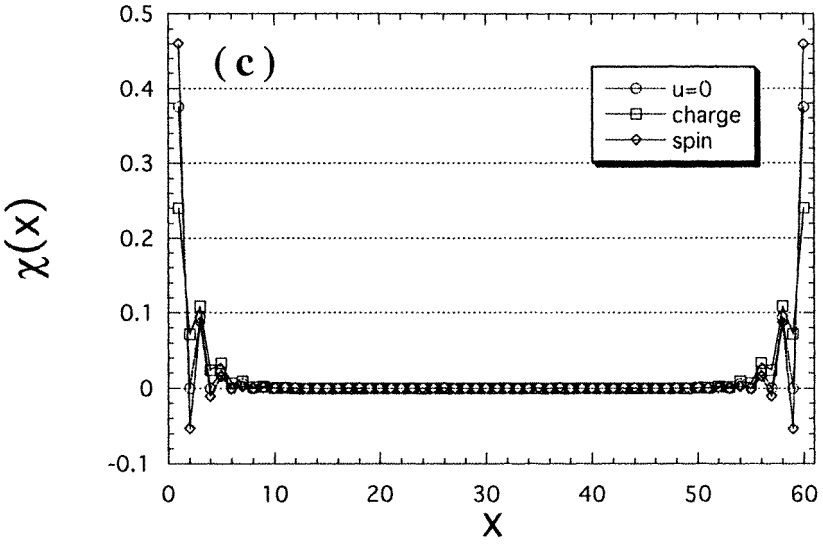

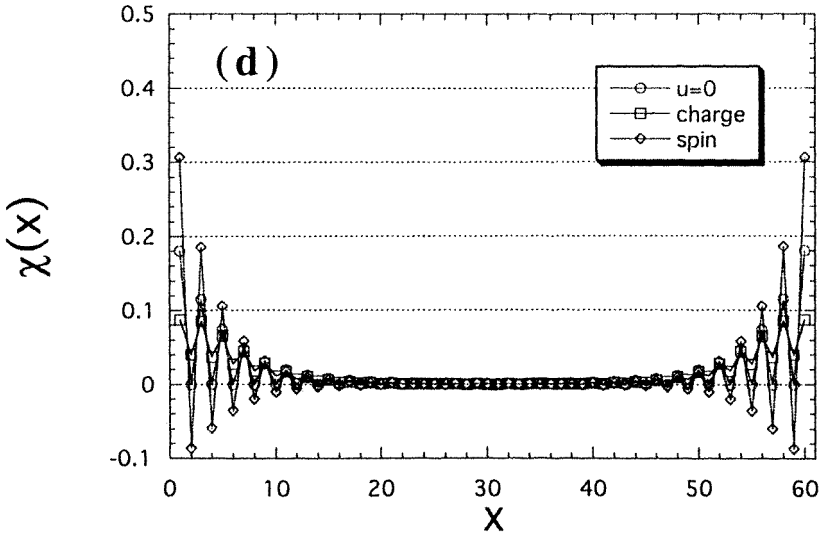

Figure 3. (Continued)

$$\mathcal{H} = -t_0 \sum_j (1 - (-1)^j \delta) \sum_{\sigma=\pm} (c^\dagger_{j\sigma} c_{j+1\sigma} + c^\dagger_{j+1\sigma} c_{j\sigma}) + 4u \sum_j \left(n_{j+} - \frac{1}{2} \right) \left(n_{j-} - \frac{1}{2} \right). \quad (4.1)$$

Here, the hopping matrix elements take two values, $t_1 \equiv t_0(1+\delta)$ and $t_2 \equiv t_0(1-\delta)$, alternately. We expect the present model with $t_1 \neq t_2$ ($t_1 > 0$, $t_2 > 0$) to have gaps in both the charge and the spin excitations at half-filling, in the thermodynamic limit. This system is expected to be a band insulator.

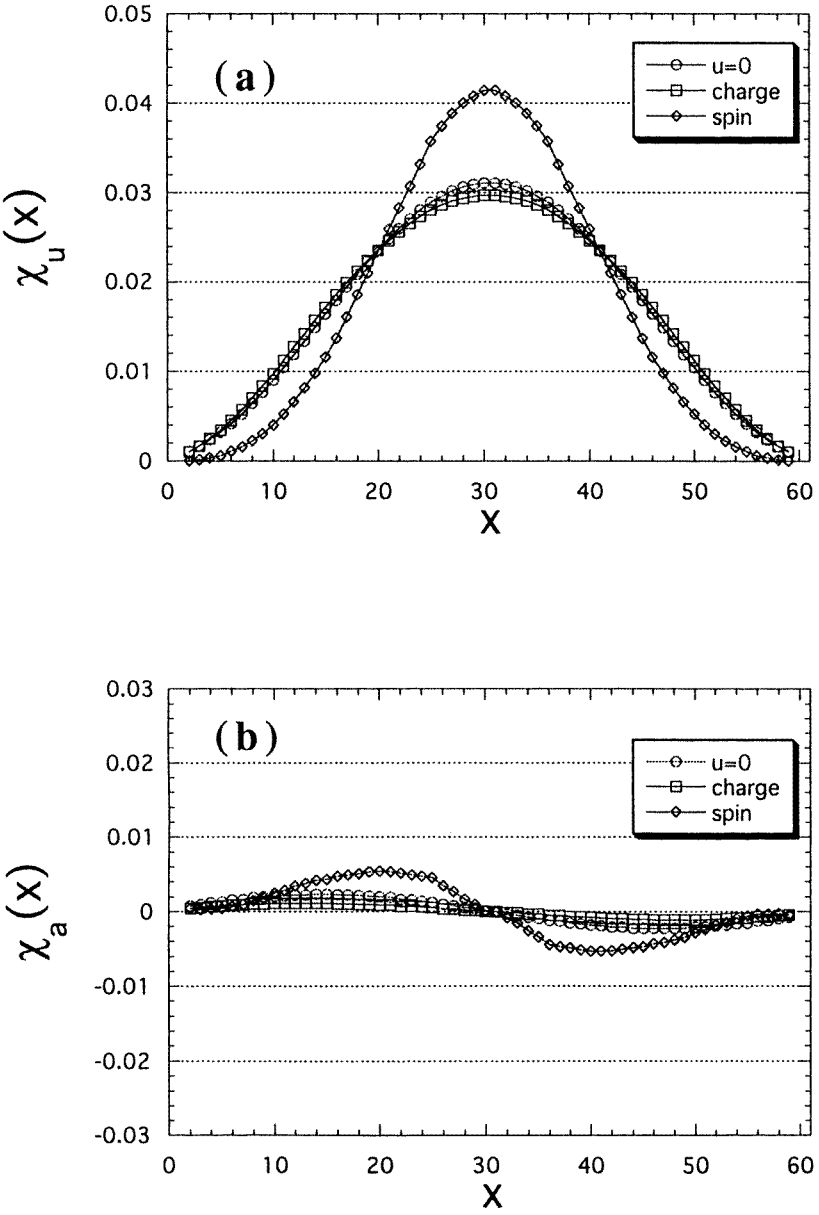

Figure 4. Uniform parts ($\chi_u(x)$) and alternating parts ($\chi_a(x)$) of the local densities on the type-A bond-alternating Hubbard open chain given in figure 3. The results for $r = 0.5$ are shown in panels (a) and (b), and those for $r = 0.8$ are shown in panels (c) and (d).

Similarly to in the previous section, we remove the operators of a site to introduce an impurity at the site. Consequently, we obtain the model of equation (4.1) with open boundaries. We only discuss the case with even L, where L denotes the chain length. We recognize that the impurities are at the sites 0 and $L + 1$. Then, we have two types of chain: **type A**: $t_1 = t$, $t_2 = t'$ and **type B**: $t_1 = t'$, $t_2 = t$, with $0 < t' \leqslant t = 1$. See figure 1.

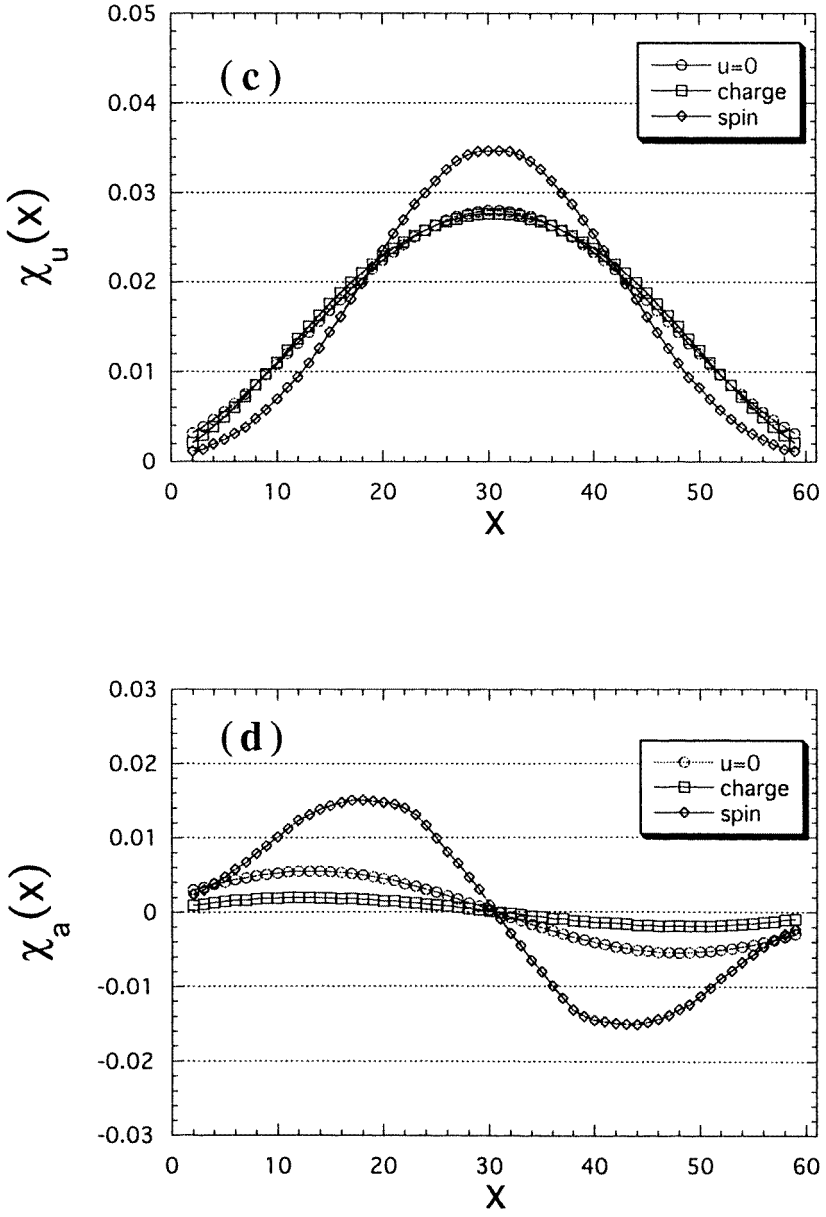

Figure 4. (Continued)

For each type of model, we calculate the reduced local densities (3.2) of the charge and spin sectors, i.e. $\chi^{(c)}(x)$ for $N_+ = \frac{L}{2} - 1$, $N_- = \frac{L}{2} - 1$ (i.e. $T^z = 1$, $S^z = 0$) and $\chi^{(s)}(x)$ for $N_+ = \frac{L}{2} + 1$, $N_- = \frac{L}{2} - 1$ (i.e. $T^z = 0$, $S^z = 1$), respectively. On the analogy of the previous section, we may recognize these quantities $\chi^{(c)}$ and $\chi^{(s)}$ as the local densities for two-particle states of holons and spinons, respectively.

In our calculations, we have taken the parameters $L = 60$, $u/t = 0.5$ and $r \equiv t'/t = 0.5, 0.8$.

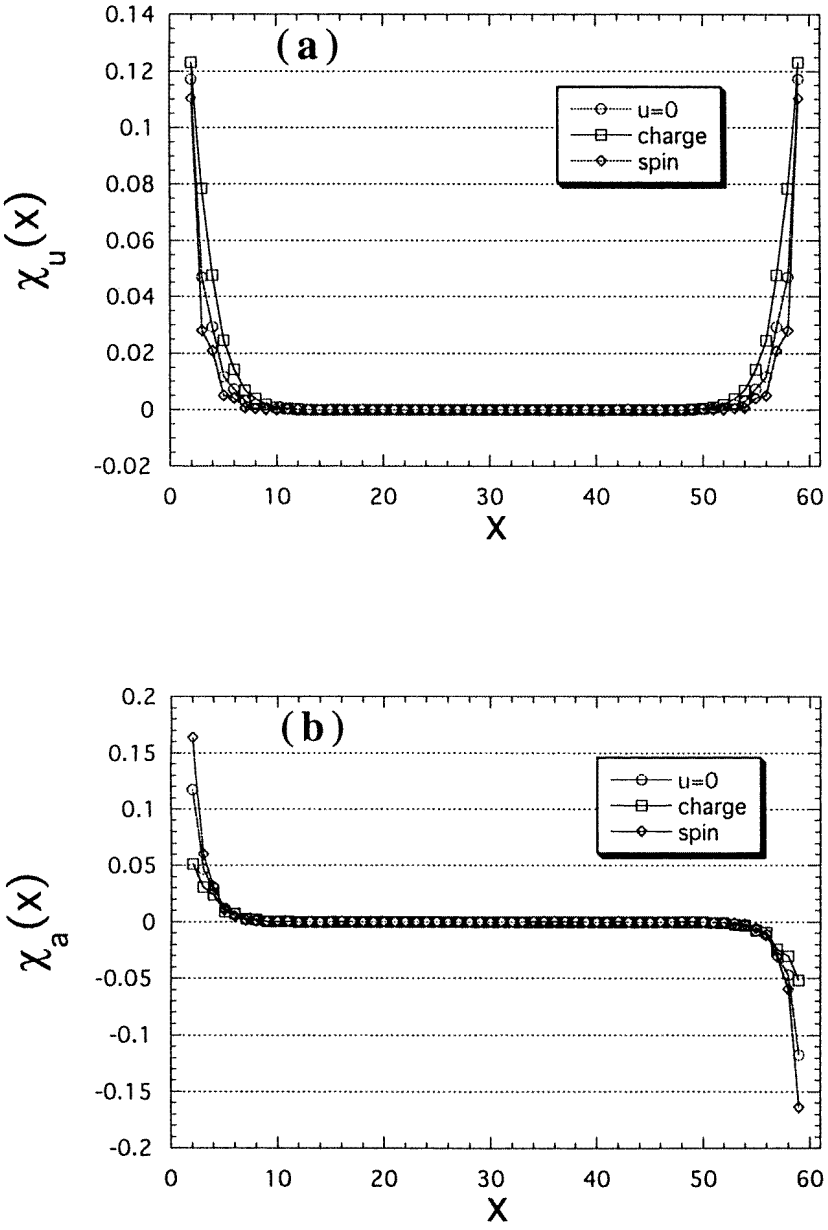

Figure 5. Uniform parts ($\chi_u(x)$) and alternating parts ($\chi_a(x)$) of the local densities on the type-B bond-alternating Hubbard chain given in figure 3. The results for $r = 0.5$ are shown in panels (a) and (b), and those for $r = 0.8$ are shown in panels (c) and (d).

In figure 3, we show the reduced local densities of the charge and spin sectors obtained from our calculations. In each figure, we also plot the results obtained with $u = 0$. We have $\chi^{(c)}(x) = \chi^{(s)}(x)$ for $u = 0$. In the type-A model, holons and spinons seem to 'feel' the repulsive potential from the edges. On the other hand, boundaries of the type-B model attract the particles.

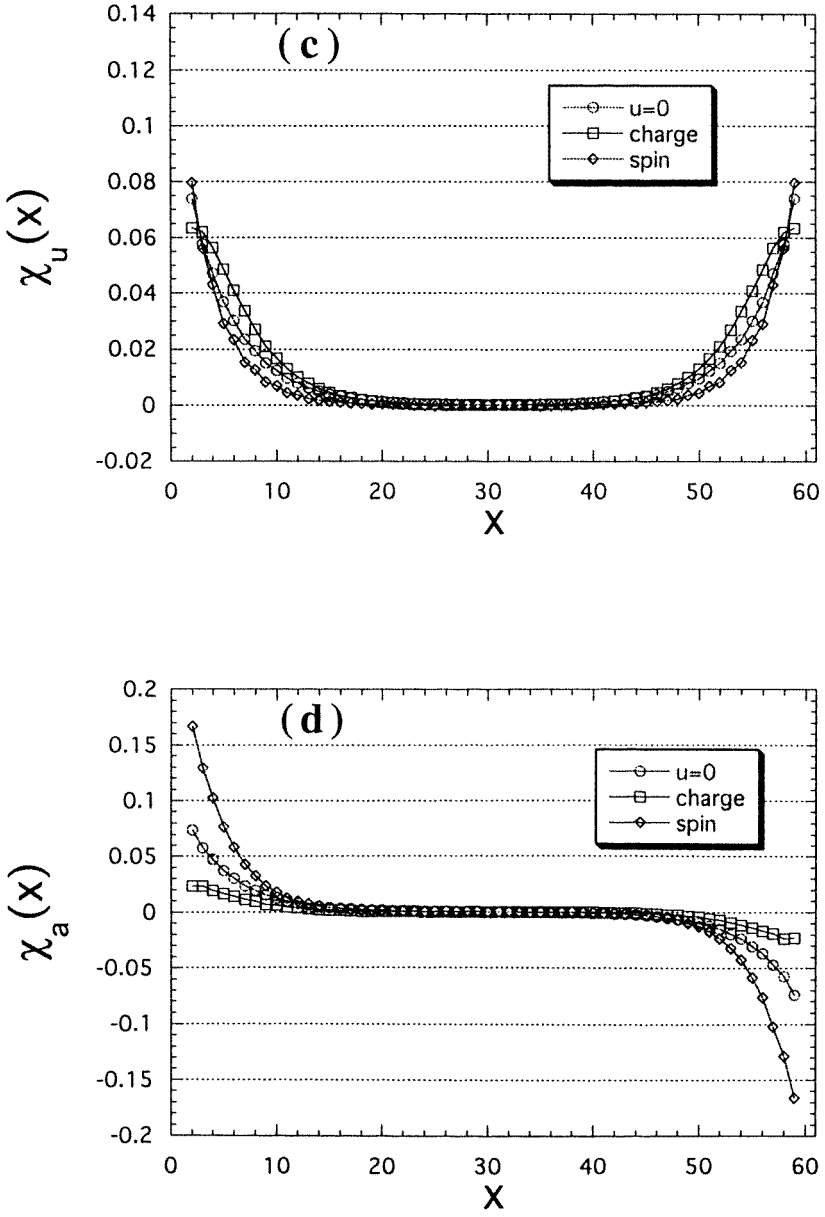

Figure 5. (Continued)

In figures 4 and 5, we show the uniform parts and the alternating parts of the local densities. At first, we focus on the type-A model (see figure 4). The uniform part of the hole density is very similar to that of the free system ($u = 0$). On the other hand, the uniform part of the spin density suggests that the boundaries repel the spinons more strongly than do the holons. The alternating part of the hole density is suppressed by the on-site Coulomb interactions, while the corresponding part of the spin density is enhanced by the Coulomb interactions. Next, we discuss the type-B model (see figure 5). Only near the boundaries do χ_u and χ_a have finite

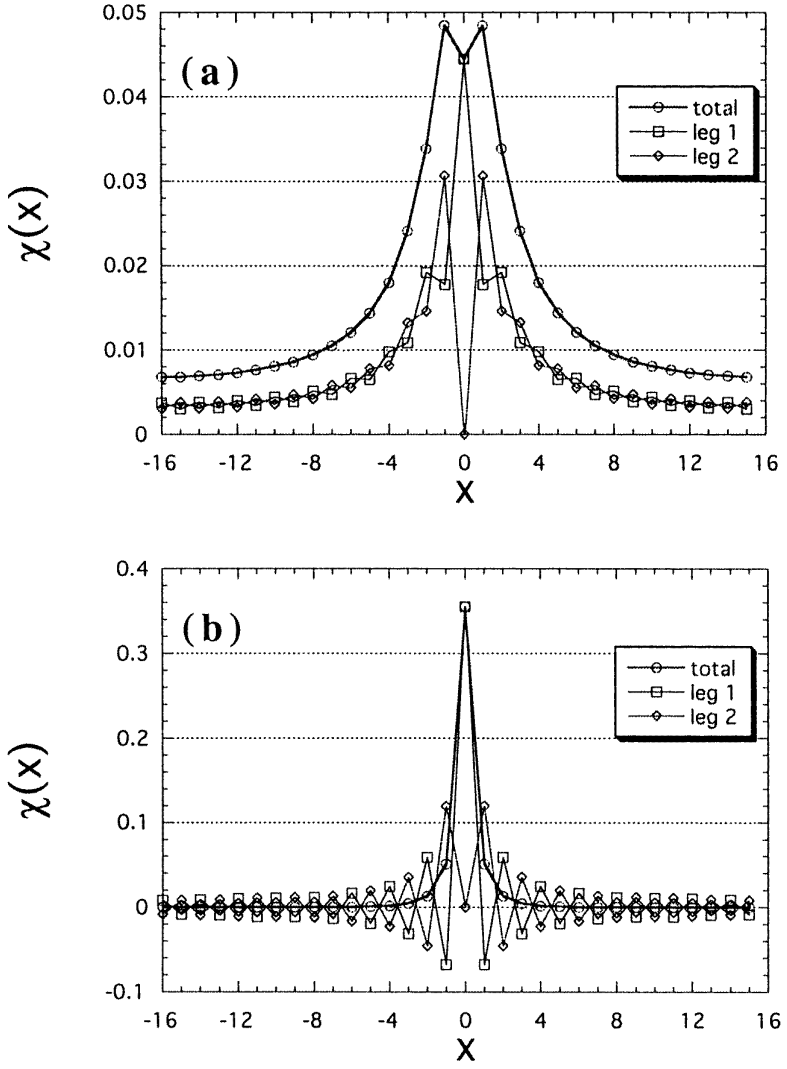

Figure 6. Local densities of the charge and spin sectors in the two-leg Hubbard ladder with a vacancy. A vacancy is located at the rung 0 on leg 2 of the ladder with $N = 63$ (i.e. $L = 32$). The charge ($\chi^{(c)}(x)$) and the spin ($\chi^{(s)}(x)$) local densities on each leg are evaluated for $T^z = \frac{1}{2}$, $S^z = 0$ (panel (a)) and for $T^z = 0$, $S^z = \frac{1}{2}$ (panel (b)), respectively.

values. This means that the boundaries trap holes and spins. The localization length of the holon near the edge is longer than that of the spinon. We expect the localization length to give the correlation length in each sector. Although our numerical results may contain a lot of finite-size effects, short localization lengths reflect the massive excitations in both sectors.

These behaviours obtained from our calculations suggest the ground-state properties of this system. Namely, the electrons on the bonds with larger hopping matrix elements tend to form charge–spin-singlet pairs, which form the ground state of the two-site Hubbard model; see appendix A. (Of course, we also have the singlet pairs on the weak bonds due to the quantum fluctuations, similarly to in the resonating-valence-bond picture [16].) Consequently, we have

unpaired electrons (i.e. holons or spinons) at the edge sites in the type-B model, which may correspond to the electrons trapped at the boundaries. On the other hand, in the type-A model, we mostly have the singlet state on the bond between sites 1 and 2 since the existence of a vacancy prevents resonance. As a result, it may be hard for unpaired electrons to stay at boundaries.

The spin sector of the present model qualitatively gives the same results as the bond-alternating Heisenberg chain; see, e.g., reference [5].

5. The two-leg ladder with a vacancy

In the present section, we consider the effects of a vacancy in the two-leg Hubbard ladder described by

$$\mathcal{H} = -t_{\parallel} \sum_{j} \sum_{a=1,2} \sum_{\sigma=\pm} (c^{\dagger}_{ja\sigma} c_{j+1a\sigma} + c^{\dagger}_{j+1a\sigma} c_{ja\sigma}) - t_{\perp} \sum_{j} \sum_{\sigma=\pm} (c^{\dagger}_{j1\sigma} c_{j2\sigma} + c^{\dagger}_{j2\sigma} c_{j1\sigma}) + 4u \sum_{j} \sum_{a=1,2} \left(n_{ja+} - \frac{1}{2} \right) \left(n_{ja-} - \frac{1}{2} \right). \tag{5.1}$$

The present model, equation (5.1), has been investigated by many authors; see, e.g., reference [17] and references cited therein. According to previous work, this system is expected to be in a charge- and spin-gapped phase for all $u > 0$ and $t_{\perp} > 0$ ($t_{\parallel} > 0$) at half-filling, in the thermodynamic limit. Moreover, the crossover from a spin-liquid Mott insulator to a band insulator at $t_{\perp}/t_{\parallel} = 2$ is expected to occur as $t_{\perp}/t_{\parallel}$ increases.

Similarly to in the previous sections, we introduce a vacancy into the ladder with L rungs under the periodic boundary condition. (We take L to be an even number.) The total number of sites in this model is given by $N = 2L - 1$.

Also in this model, we calculate the reduced local densities (3.2) of the charge and spin sectors; $\chi^{(\mathrm{c})}(x)$ for $N_+ = L - 1$, $N_- = L - 1$ (i.e. $T^z = \frac{1}{2}$, $S^z = 0$) and $\chi^{(\mathrm{s})}(x)$ for $N_+ = L + 1$, $N_- = L - 1$ (i.e. $T^z = 0$, $S^z = \frac{1}{2}$), respectively. Here, $\chi^{(\mathrm{c})}(x) = \chi^{(\mathrm{s})}(x)$ holds for $u = 0$. Then, we may recognize that $\chi^{(\mathrm{c})}$ (or $\chi^{(\mathrm{s})}$) describes the local density of the one-holon (or one-spinon) state.

In our calculations, we take $N = 63$ (i.e. $L = 32$), $u = 0.5$, $t_{\parallel} = 0.5$ and $t_{\perp} = 1$ (i.e. $t_{\perp}/t_{\parallel} = 2$). We introduce an impurity at the rung 0 on the leg 2. We have to identify the rung $-L/2$ as the rung $L/2$ due to the periodic boundary condition.

In figure 6, we plot the reduced densities on the two legs. We also show the total density on each rung. In the charge (or spin) sector, a charge (or spin) 'moment' is enhanced around the vacancy, in terms of the SO(4) symmetry.

In figure 7, we show uniform and staggered (i.e. alternating) parts of the local densities on each leg. The uniform part on a leg gets larger near the impurity. The fact that the staggered parts on the two legs take opposite signs comes from the alternate oscillation of the densities on the legs.

The enhancement of the moment around the vacancy suggests the local properties of the ground state of the present model. Namely, we can expect a pair of electrons to mostly form an SO(4)-singlet dimer at each rung. In each dimer, the 'spinon and antispinon' or 'holon and antiholon' confine one another to realize the singlet state. (Refer to appendix A.) As a result, we have an unpaired holon or spinon with finite moments when we remove a site and the electrons at that site.

The spin sector of the present model qualitatively gives the same results as the two-leg Heisenberg ladder with nonmagnetic impurities; see, e.g., references [1, 5].

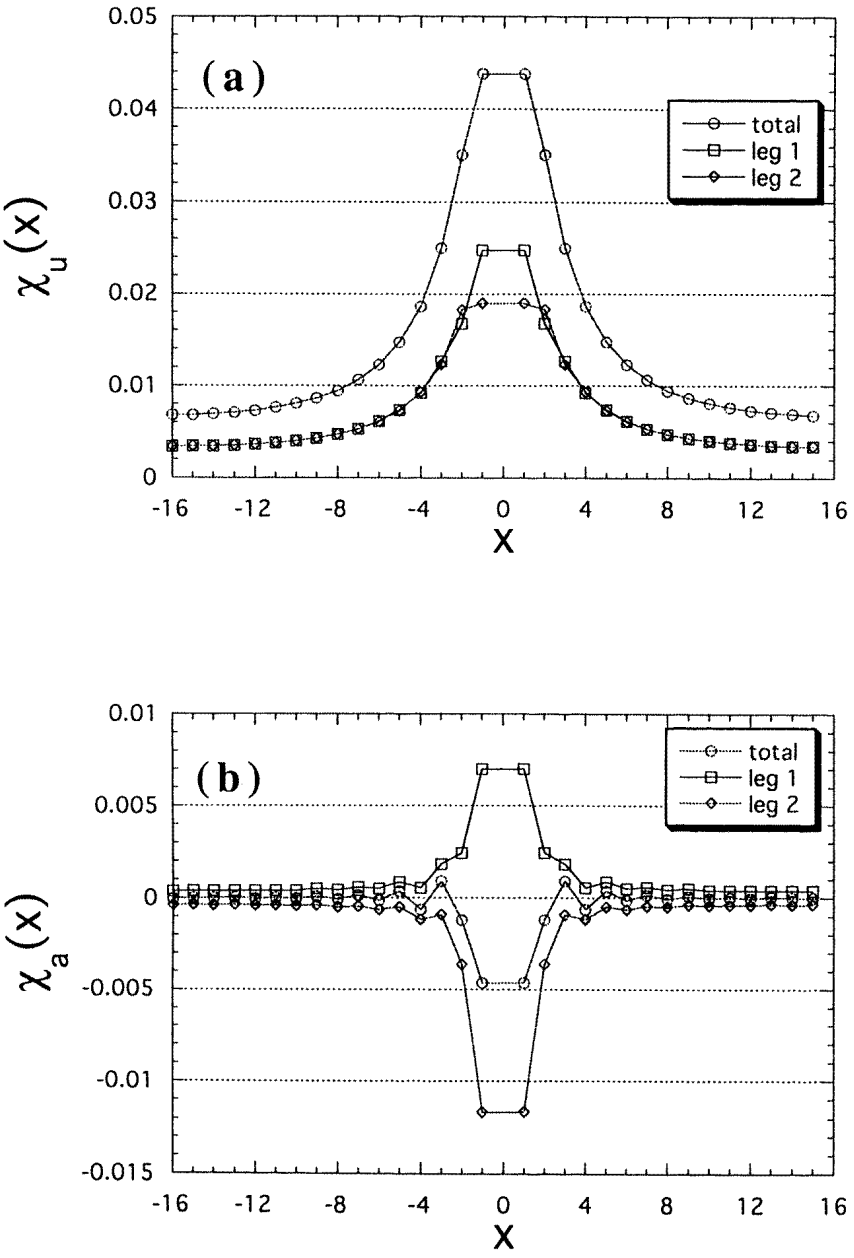

Figure 7. Uniform parts ($\chi_u(x)$) and alternating parts ($\chi_a(x)$) of the local densities on the two-leg Hubbard ladder given in figure 6. The results for charge densities are given in panels (a) and (b), and those for spin densities are given in panels (c) and (d).

6. The zigzag ladder with a vacancy

In the present section, we consider the effects of chargeless and spinless impurities in the zigzag Hubbard ladder described by

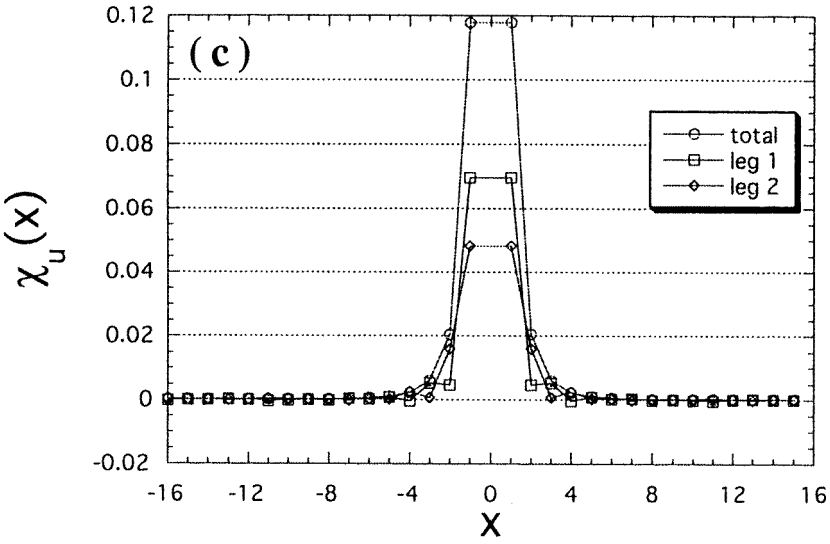

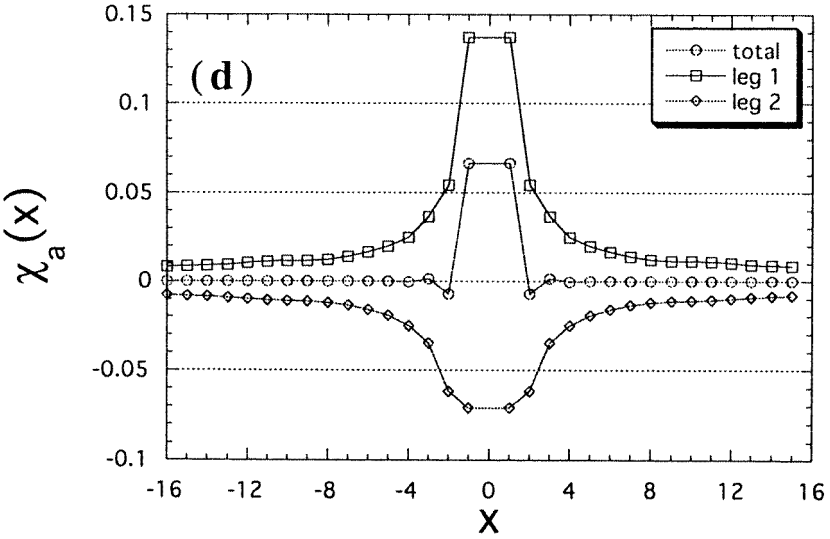

Figure 7. (Continued)

$$\mathcal{H} = -t_1 \sum_j \sum_{\sigma=\pm} (c^\dagger_{j\sigma} c_{j+1\sigma} + c^\dagger_{j+1\sigma} c_{j\sigma}) - t_2 \sum_j \sum_{\sigma=\pm} (c^\dagger_{j\sigma} c_{j+2\sigma} + c^\dagger_{j+2\sigma} c_{j\sigma}) + 4u \sum_j \left(n_{j+} - \frac{1}{2}\right)\left(n_{j-} - \frac{1}{2}\right). \tag{6.1}$$

The present model, equation (6.1), has also been discussed by many authors; see, e.g., reference [18] and references cited therein. According to previous work, we have a spin-

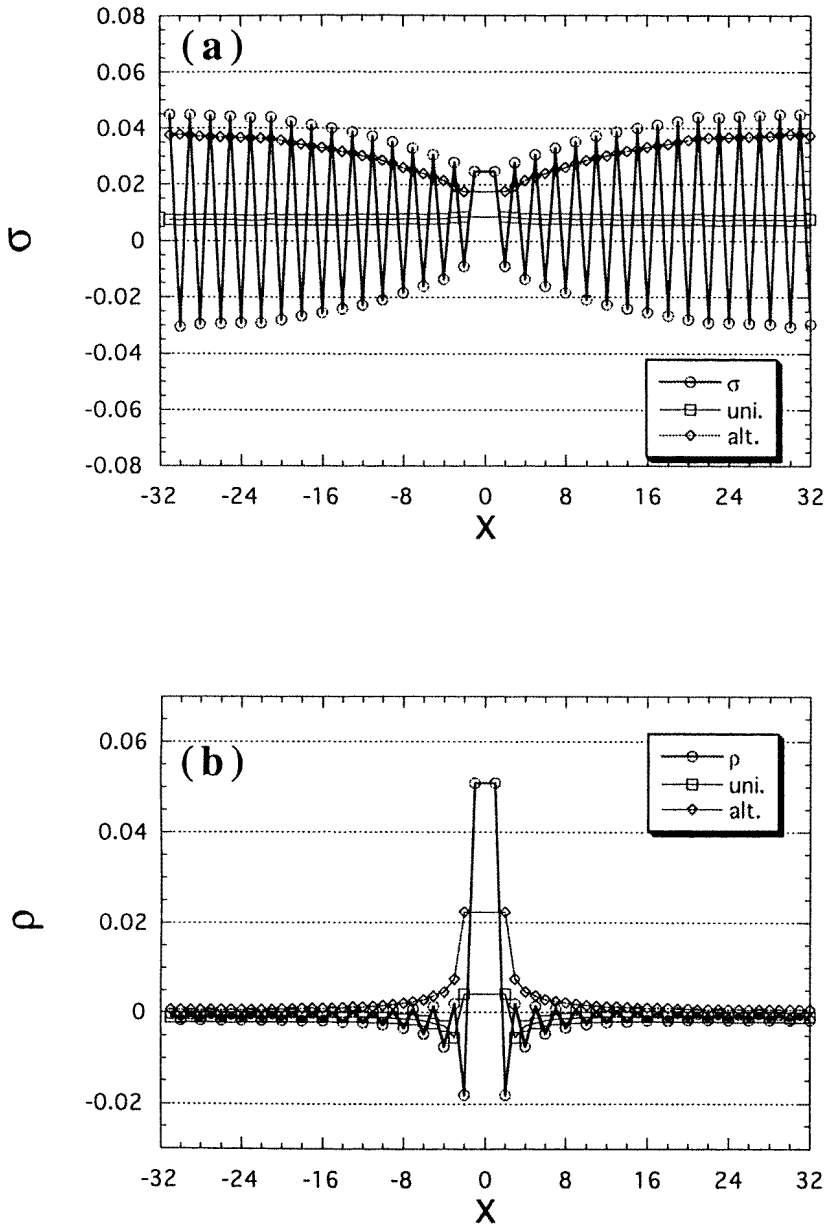

Figure 8. Local densities of the electron number ($\rho(x)$) and the magnetization ($\sigma(x)$) in the zigzag Hubbard ladder with a vacancy. A vacancy is located at the site 0 of the ladder with $N = 63$ (i.e. $L = 64$). In panels (a) and (b), we give $\sigma(x)$ and $\rho(x)$ for $\Delta N = 0$, $S^z = \frac{1}{2}$, respectively. We give the local electron numbers for $\Delta N = -1$, $S^z = 0$ and for $\Delta N = +1$, $S^z = 0$ in panels (c) and (d), respectively.

gapless phase with a charge gap for small $u > 0$ and $|t_2| < t_{2c}$ ($t_1 > 0$) at half-filling in the thermodynamic limit. (For $u \to 0$, t_{2c} goes to $0.5t_1$.) This phase is expected to be a Mott insulator with a gapless spin excitation. We concentrate on this phase in our discussions.

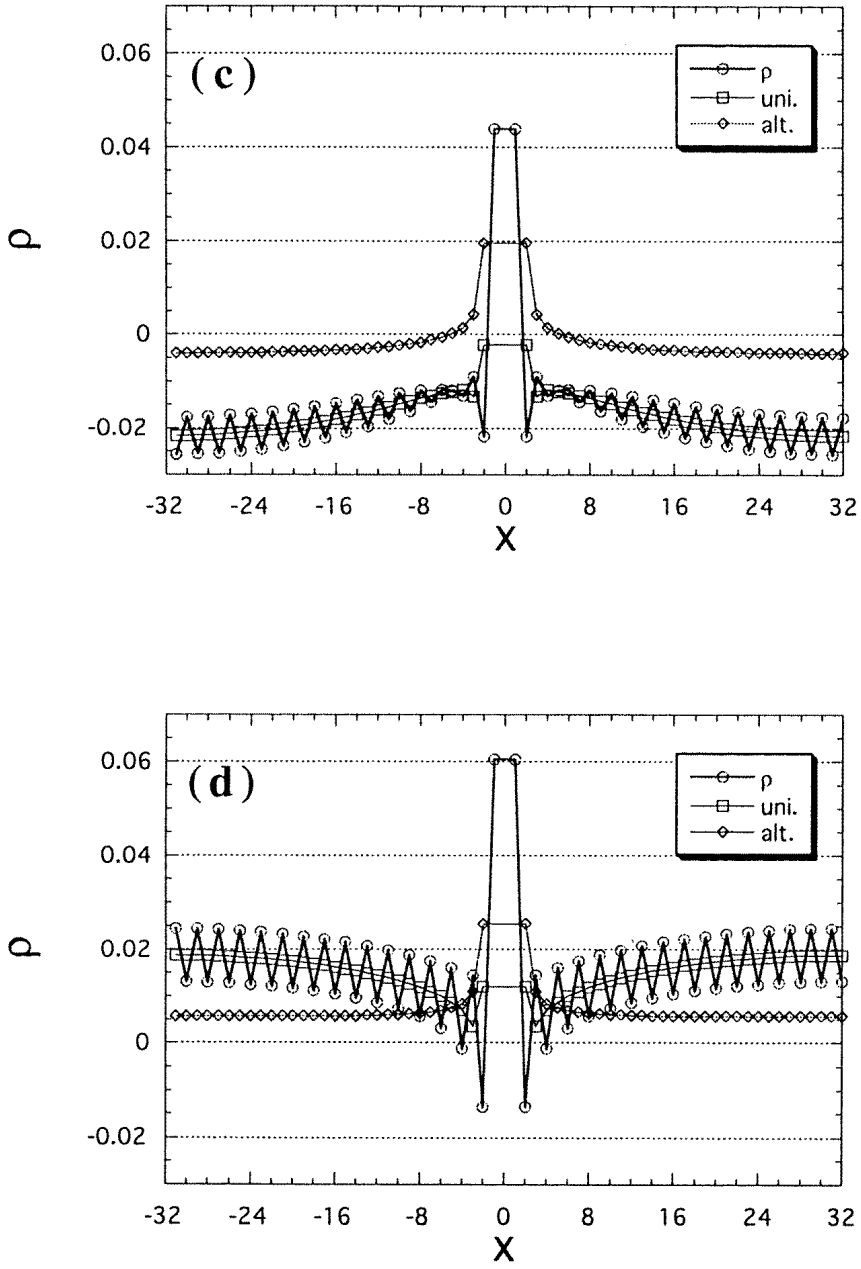

Figure 8. (Continued)

In the same way as in the previous sections, we introduce a vacancy into the zigzag ladder with L sites (where L is an even number) to obtain a system with $N = L - 1$ sites.

We remark that this model does not have particle–hole symmetry or SO(4) symmetry. That is, we cannot convert the results for $T^z = \frac{1}{2}$ to results for $T^z = -\frac{1}{2}$ by the particle–hole transformation and T is not a good quantum number. However, S, S^z and T^z are still good

quantum numbers, since the present model has $U(1)_{\rm charge} \times SU(2)_{\rm spin}$ symmetry. Instead of using T^z, we take the quantity $\Delta N \equiv -2T^z$ in this section, which denotes the deviation of the electron number from the half-filling value. Taking this situation into account, we evaluate the following quantities for the present model, equation (6.1):

$$\begin{aligned} \rho(x) &= \langle n_{x+} + n_{x-} - 1 \rangle \\ \sigma(x) &= \frac{1}{2}\langle n_{x+} - n_{x-} \rangle \end{aligned} \tag{6.2}$$

where $\rho(x)$ and $\sigma(x)$ are just the charge density and the spin density at site x. For $\Delta N = 0$, $S^z = \frac{1}{2}$, we evaluate $\rho(x)$ and $\sigma(x)$. For $\Delta N = \pm 1$ and $S^z = 0$, $\rho(x)$ is evaluated.

In our calculations, we take the parameters $N = 63$ (i.e. $L = 64$), $u = 0.5$, $t_1 = 1$ and $t_2 = 0.25$. We introduce a vacancy at the site 0. We have to identify the site $-L$ as the site L because of the periodic boundary condition.

In figure 8, we show the results obtained from our calculations. The spin density for $\Delta N = 0$, $S^z = \frac{1}{2}$ behaves similarly to the corresponding spin density in the Hubbard open chain with an odd number of sites. On the other hand, an electron bound state seems to emerge near the vacancy. In particular, the charge density for $\Delta N = 0$, $S^z = \frac{1}{2}$ is similar to the local densities in the bond-alternating model of type B. Also, in the cases with $\Delta N = \pm 1$, $S^z = 0$, electrons may be trapped near the vacancy. However, away from the vacancy, the electron densities for these cases show a similar behaviour to those for the Hubbard open chain with odd numbers of sites. The chargeless and spinless impurity attracts charges, while spins almost recognize the vacancy as a free end.

The behaviours of the charge and the spin densities away from the vacancy suggest that the bulk properties of the present model are essentially the same as those of the ordinary Hubbard model on a chain. That is, the present model with our parameters is in a spin-gapless phase with a charge gap, as we had expected.

7. Summary

In the present paper, we study the effects of vacancies (i.e. chargeless and spinless impurities) in the Hubbard models on several chains and ladders using the quantum Monte Carlo method. We focus on the properties near half-filling.

In section 4, we have introduced vacancies into the bond-alternating Hubbard open chain. This system is expected to be a band insulator at half-filling. The impurity repels (or attracts) holons and spinons in the type-A (or type-B) model. That is, when the first link after the chain end has a larger (or smaller) hopping matrix element (i.e. t), the vacancy behaves as an attractive potential (or a repulsive potential).

In section 5, we have put an impurity at a site in the two-leg Hubbard ladder. We have set this model in the crossover region between a band insulator phase and a spin-liquid Mott insulator phase. The vacancy seems to attract holons and spinons. In other words, we can recognize the enhanced moment as an unpaired holon or spinon since a charge–spin-singlet dimer is almost localized on each rung.

In section 6, we have set an impurity at a site in the zigzag Hubbard ladder. We have concentrated on a Mott insulator phase with a gapless spin excitation in this model. The vacancy behaves as free ends for the spin sector. On the other hand, charges seem to be trapped by the impurity.

Quantitative discussions of each model will be reported elsewhere in the near future.

Acknowledgments

All of the numerical calculations in the present paper were performed on a DEC300/300LX (OSF/1) workstation installed at RIKEN. The author is supported by the Special Postdoctoral Researchers Programme in RIKEN. He thanks Y Asakawa for her continual and cordial encouragement.

Appendix A

In the present section, we briefly summarize the eigenstates of the two-site Hubbard model from the viewpoint of the SO(4) symmetry.

Next, we describe the Hamiltonian of the two-site Hubbard model by

$$\mathcal{H}_2 = -t\,(c^\dagger_{1+}c_{2+} + c^\dagger_{2+}c_{1+} + c^\dagger_{1-}c_{2-} + c^\dagger_{2-}c_{1-}) + 4u\left(n_{1+} - \frac{1}{2}\right)\left(n_{1-} - \frac{1}{2}\right) + 4u\left(n_{2+} - \frac{1}{2}\right)\left(n_{2-} - \frac{1}{2}\right). \tag{A.1}$$

We can write down the generators of the SO(4) symmetry of the two-site model as follows:

$$S^+ = \sum_{j=1,2} c^\dagger_{j+}c_{j-} \qquad S^- = (S^+)^\dagger \qquad S^3 = \frac{1}{2}\sum_{j=1,2}(n_{j+} - n_{j-}) \tag{A.2}$$

$$T^+ = \sum_{j=1,2} (-1)^j c_{j+}c_{j-} \qquad T^- = (T^+)^\dagger \qquad T^3 = \frac{1}{2}\sum_{j=1,2}(1 - n_{j+} - n_{j-}). \tag{A.3}$$

Due to the SO(4) symmetry, we can label all 16 eigenstates of this model (A.1) as follows:

$$S = 0,\ T = 1\text{:}\ \left\{|00\rangle,\ \frac{1}{\sqrt{2}}(|0\pm\rangle - |\pm 0\rangle),\ -|\pm\pm\rangle\right\} \qquad E = +2u$$

$$S = 1,\ T = 0\text{:}\ \left\{|{+}{+}\rangle,\ \frac{1}{\sqrt{2}}(|{+}{-}\rangle + |{-}{+}\rangle),\ |{-}{-}\rangle\right\} \qquad E = -2u$$

$$S = \frac{1}{2},\ T = \frac{1}{2}\text{:}\ \left\{\begin{array}{l} \frac{1}{\sqrt{2}}(|{+}0\rangle - |0{+}\rangle),\ \frac{-1}{\sqrt{2}}(|\pm{+}\rangle + |{+}\pm\rangle) \\ \frac{1}{\sqrt{2}}(|{-}0\rangle - |0{-}\rangle),\ \frac{-1}{\sqrt{2}}(|\pm{-}\rangle + |{-}\pm\rangle) \end{array}\right\} \qquad E = +t$$

$$S = \frac{1}{2},\ T = \frac{1}{2}\text{:}\ \left\{\begin{array}{l} \frac{1}{\sqrt{2}}(|{+}0\rangle + |0{+}\rangle),\ \frac{1}{\sqrt{2}}(|\pm{+}\rangle - |{+}\pm\rangle) \\ \frac{1}{\sqrt{2}}(|{-}0\rangle + |0{-}\rangle),\ \frac{1}{\sqrt{2}}(|\pm{-}\rangle - |{-}\pm\rangle) \end{array}\right\} \qquad E = -t$$

$$S = 0,\ T = 0\text{:}\ \cos\theta|\alpha\rangle - \sin\theta|\beta\rangle\ (\equiv|\mathrm{A}\rangle) \qquad E = +2\sqrt{u^2 + t^2}$$

$$S = 0,\ T = 0\text{:}\ \sin\theta|\alpha\rangle + \cos\theta|\beta\rangle\ (\equiv|\mathrm{B}\rangle) \qquad E = -2\sqrt{u^2 + t^2}$$

with $\tan 2\theta = t/u$ and

$$|\alpha\rangle = \frac{1}{\sqrt{2}}(|\pm 0\rangle + |0\pm\rangle) \qquad |\beta\rangle = \frac{1}{\sqrt{2}}(|{+}{-}\rangle - |{-}{+}\rangle) \tag{A.4}$$

where each of the states $|\alpha\rangle$ and $|\beta\rangle$ has quantum numbers $S = 0$, $T = 0$. In the above equations, E denotes the energy eigenvalue and the state vectors are defined by, e.g., $|{+}{-}\rangle \equiv c^\dagger_{1+}c^\dagger_{2-}|\mathrm{vac}\rangle$ etc, in terms of the vacuum, $|\mathrm{vac}\rangle$, of the no-electron state.

That is, the ground state of the present model is given by $|\mathrm{B}\rangle$, which is a spin-singlet and charge-singlet state.

References

[1] Sandvik A W, Dagotto E and Scalapino D J 1997 *Phys. Rev.* B **56** 11 701
[2] Motome Y, Katoh N, Furukawa N and Imada M 1996 *J. Phys. Soc. Japan* **65** 1949
[3] Nagaosa N, Furusaki A, Sigrist M and Fukuyama H 1996 *J. Phys. Soc. Japan* **65** 3724
[4] Mikeska H-J, Neugebauer U and Schollwöck U 1997 *Phys. Rev.* B **55** 2955
[5] Laukamp M, Martins G B, Gazza C, Malvezzi A L, Dagotto E, Hansen P M, López A C and Riera J 1998 *Phys. Rev.* B **57** 10 755
[6] Heilmann O J and Lieb E H 1971 *Ann. New York Acad. Sci.* **172** 583
[7] Essler F H L and Korepin V E 1994 *Nucl. Phys.* B **426** 505
[8] Suzuki M 1976 *Prog. Theor. Phys.* **56** 1454
[9] Sorella S, Tosatti E, Baroni S, Car R and Parrinello M 1988 *Int. J. Mod. Phys.* B **2** 993
[10] White S R, Scalapino D J, Sugar R L, Loh E Y, Gubernatis J E and Scalettar R T 1989 *Phys. Rev.* B **40** 506
[11] Imada M and Hatsugai Y 1989 *J. Phys. Soc. Japan* **58** 3752
[12] Schulz H 1985 *J. Phys. C: Solid State Phys.* **18** 581
[13] Asakawa H 1998 *J. Phys.: Condens. Matter* at press
[14] Bedürftig G, Brendel B, Frahm H and Noack R M 1998 *Preprint* cond-mat/9805123
[15] Asakawa H and Suzuki M 1997 *J. Phys. A : Math. Gen.* **30** 3741
[16] Anderson P W 1987 *Science* **235** 1196
[17] Noack R M, White S R and Scalapino D J 1996 *Physica* C **270** 281
[18] Daul S and Noack R M 1998 *Phys. Rev.* B **58** 2635